Original Article

www.jmss.mui.ac.ir

Multi-scale Morphological Image Enhancement of Chest Radiographs by a Hybrid Scheme

Fatemeh Shahsavari Alavijeh, Homayoun Mahdavi-Nasab

Department of Electrical Engineering, Najafabad Branch, Islamic Azad University, Najafabad, Isfahan, Iran

Submission: 16-09-2014 Accepted: 30-12-2014

ABSTRACT

Chest radiography is a common diagnostic imaging test, which contains an enormous amount of information about a patient. However, its interpretation is highly challenging. The accuracy of the diagnostic process is greatly influenced by image processing algorithms; hence enhancement of the images is indispensable in order to improve visibility of the details. This paper aims at improving radiograph parameters such as contrast, sharpness, noise level, and brightness to enhance chest radiographs, making use of a triangulation method. Here, contrast limited adaptive histogram equalization technique and noise suppression are simultaneously performed in wavelet domain in a new scheme, followed by morphological top-hat and bottom-hat filtering. A unique implementation of morphological filters allows for adjustment of the image brightness and significant enhancement of the contrast. The proposed method is tested on chest radiographs from Japanese Society of Radiological Technology database. The results are compared with conventional enhancement techniques such as histogram equalization, contrast limited adaptive histogram equalization, Retinex, and some recently proposed methods to show its strengths. The experimental results reveal that the proposed method can remarkably improve the image contrast while keeping the sensitive chest tissue information so that radiologists might have a more precise interpretation.

Key words: *Chest radiographs image enhancement, morphological filtering, multiscale image processing, wavelet transform*

INTRODUCTION

Despite recent advances in cross-sectional imaging of the thorax, conventional chest radiography remains as the main test in primary diagnosis of many diseases. In most cases, it is the first and only diagnostic imaging test done for patients to approve or reject having abnormal chest. An enormous amount of information about the condition of the patient can be extracted from a chest radiograph.[1] However, its interpretation is immensely challenging.

The chest's large field of view imposes challenging constraints including the wide latitude of X-ray transmission through the anatomical structures that results in poor dynamic range and limitation in depiction of minute differences associated with subtle low-contrast features in the image. It also increases the contribution of scattered radiation to the image and so has the deleterious effects of increasing image noise and reduced inherent contrast.[1,2]

The accuracy of the diagnostic process is greatly influenced by image processing algorithms.[3] Image processing allows for significant enhancement of the visibility of the details. Hence, image enhancement is indispensable in order to improve the perception of chest image information. A wide variety of procedures are existing for enhancing the digital radiographic images which vary from the simple classic contrast enhancement techniques like histogram equalization (HE) to mathematical signal processing techniques.[4,5] The clinical importance of chest radiograph, accompanied by its complicated nature, has been the prime motivation in most of the computer algorithms for assisting radiologists in investigating chest images. Nowadays, almost all digital X-ray machines have been introduced through additional processing in order to have a larger dynamic range and contrast enhancements.[1]

In this study, an attempt has been made to develop a technique for improving the radiograph parameters such as contrast, sharpness, noise level, and brightness simultaneously. The main goals of our research are to provide better representation of lung details while improving the contrast. To this end, novel simultaneous adaptive local contrast equalization and noise suppression in digital wavelet domain is proposed. A mixed top-hat and bottom-hat morphological postprocessing accomplishes

Address for correspondence:
Dr. Homayoun Mahdavi-Nasab, Department of Electrical Engineering, Najafabad Branch, Islamic Azad University, Najafabad, Isfahan, Iran.
E-mail: mahdavinasab@iaun.ac.ir.

the process. The method discussed here may act as the preprocessing stage to supply improved input data for further processing applications in computer-aided diagnosis systems in order to enhance the diagnosis performance.[6]

The remainder of this paper is organized as follows. The next section describes some related works. In section 3, the proposed hybrid enhancement method is presented. A brief description of wavelet transformation is given in section 3.1. Noise reduction by nonlinear thresholding and contrast limited adaptive histogram equalization (CLAHE) are described in sections 3.2 and 3.3. Final processing steps, including the implementation of a combination of morphological filters are given in sections 3.4 and 3.5. Section 4 presents the results. Finally, conclusions are drawn in section 5.

LITERATURE REVIEW

The enhancement techniques can be generally classified into two types: Intensity-based processing and feature-based processing. The most common intensity based techniques are contrasted stretching[7] and HE.[8,9] Some HE modification approaches are bi-histogram equalization,[10] multi-peak HE,[11] multi-histogram equalization,[12] adaptive histogram equalization (AHE),[13] and CLAHE.[14] Pizer *et al*. intended to evaluate the clinical application of CLAHE to chest computer tomography (CT) images by demonstrating fast implementation ability.[15] Furthermore, a statistically significant improvement in detection performance for simulated speculations in dense mammograms with CLAHE was reported.[16] CLAHE is applied to digital chest radiographs to enhance contrast and the boundary artifact is reduced by means of background subtraction prior to applying the CLAHE algorithm.[17]

Sherrier and Johnson proposed a regionally AHE method to enhance chest radiographs, which perform only at the grid points over the mediastinum and subdiaphragm, but the grid points over the lung field are not processed.[4] Chest radiograph image is divided into three subregions according to the gray-level properties, and a piecewise linear transformation model is applied to enhance the contrast.[18] The performance of HE, AHE, and CLAHE is compared.[19]

In feature-based enhancement category the classic unsharp masking technique is commonly used.[20-23] Three steps consist of the median filter for removing noise, followed by unsharp mask filter for sharpening and CLAHE are implemented.[23] Mean and median filtering are proposed for noise removal.[24] A linear phase, high-frequency emphasis finite impulse response filter is offered to amplify high-frequency features. Then, HE is applied on chest radiographs.[25] Temporal subtraction aims to suppress normal structures in chest radiographs resulting in the visibility of abnormalities.[26] A parameterized logarithmic image processing method based on Laplacian of Gaussian (LoG) filtering is introduced to enhance lung nodules.[27] Hessian-LoG filter is developed to enhance dot-like objects.[28] Shuyue and Ling proposed two-scale Retinex method. In wavelet domain, wavelet coefficients are manipulated for enhancement.[5,30-35] A sigmoid-type transference is proposed to adjust wavelet detail coefficients (for contrast improving chest radiographs, mammograms, and chest CT images).[34] In this paper, Retinex method, unsharp masking technique[23] and sigmoid-transfer are implemented in order to compare results. The multi-scale contrast amplification algorithm based on the concept of the Laplacian pyramid is presented to the problem of detail contrast enhancement.[36] A review of twelve different techniques based on local equalization, sharpening, fuzzy set, neural network was shortly discussed.[37] In order to avoid anatomical division error, we are looking for an approach which does not require any priori anatomy information and is able to be applied to most digital radiographic images.[4,18,20,35]

METHODS

The method starts by decomposing images using discrete wavelet transform (DWT). Image denoising is done by processing the details coefficients using BayesShrink thresholding. Eliminating as much noise as possible is followed by image linearly sharpening based on an appropriate amplification of the high-frequency details coefficients.

The low-frequency components form the background or base of the image that is generally smooth and low contrast. However, they are usually kept unaltered due to the risk of image deterioration; although containing much of the energy distribution. In our scheme, CLAHE is applied to normalized low-frequency components of chest image. Less potential to produce noise and visual artifacts are among the benefits of this method.

After applying inverse DWT, some of the highest and lowest intensities of normalized images are clipped to reduce the overall opaque. Finally, a linear combination of normalized input image and the morphologically filtered ones are employed to achieve better appearance for bright and dark features. Top-hat and bottom-hat filtering are generally used together to enhance contrast using a small and equal structuring element (SE). Here, in a different manner, the size of disk-shaped SE was selected large and unequal; greater SE for the bottom-hat filters. This made us possible to adjust the image brightness and contrast more uniformly. Indeed, in this method the dark features were almost strengthened twice the bright ones. Figure 1 shows the block diagram of the proposed enhancement process.

Multi-scale Processing

Multi-resolution image representations facilitate analysis of images like a mathematical microscope. Various anatomic

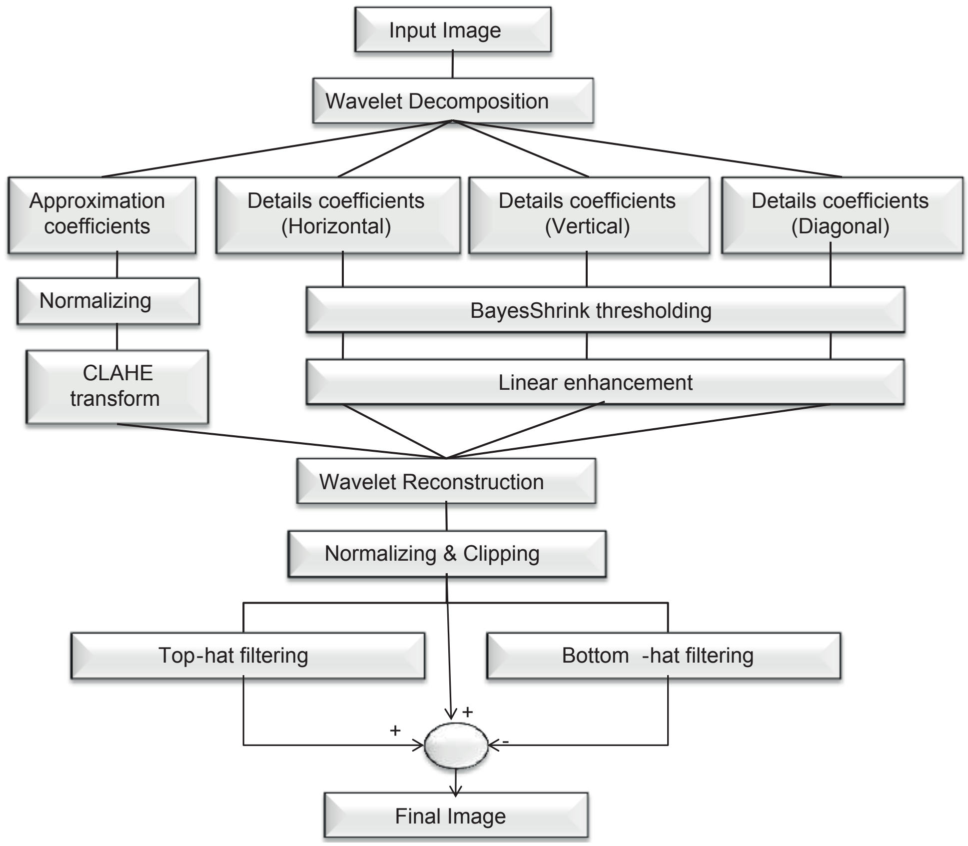

Figure 1: Block diagram of the proposed enhancement process

structures of chest radiograph have very different texture patterns and optical densities. Multi-resolution WT seems to be appropriate to analyze such images. Fast implementation of DWT enables real-time processing capability.

Wavelet transform can be classified based on the orthogonality. Decomposing the signal on a wavelet orthogonal basis gives a compact, efficient representation of the signal, which its information is not redundant. The 2-level orthogonal wavelet decomposition of chest radiographs is shown in Figure 2. The isolation of noise from the signal might be achieved more effectively by orthogonal WT. The use of an orthogonal basis implies the use of DWT due to the existence of a countable orthogonal basis set in the separable Hilbert space. The most known family of orthogonal wavelets is the Daubechies family. In this study, wavelet transform employs Daubechies' least asymmetric compactly-supported wavelet with eight vanishing moments.[38] Daubechies has proposed it as the modifications of Daubechies orthogonal wavelets with increased symmetry. The symmetry is useful in avoiding dephasing in image processing. It should be noted that linear-phase implies nonorthogonality.

Denoising and Sharpening

In order to avoid noise increasing during features enhancement in image, the three wavelet detail bands coefficients (horizontal, vertical, diagonal) are firstly processed by BayesShrink thresholding[39] in the four scales of decomposition. BayesShrink is an adaptive data-driven threshold in a Bayesian framework. It is appropriate to improve useful high-frequency information using a simple linear remapping function. The amplitude of details coefficients in the first scale is amplified through multiplying it by a constant amplification factor in order to visualize the fine details as:

$$D(i,j) = \alpha\, D(i,j), \alpha \geq 1. \quad (1)$$

The constant amplification factor (α) should not be chosen such that it makes a too sharp image. The constant amplification factor was set here to 1.68. Furthermore, in order to preserve the order of contrasts of structures, the amplification factor has been selected to be constant. Whereas in some articles,[33,34] a nonlinear transfer function was employed to modify the details coefficients that seem to create a false image harmonic impression slightly.

Contrast Limited Adaptive Histogram Equalization

Histogram equalization improves contrast by flattening the histogram. Since HE operates uniformly on the entire images, it isn't able to achieve the local contrast. To overcome such drawbacks, generalization of HE technique has been proposed, beginning with AHE. AHE partition the image into the multiple contextual regions. There is a major drawback that is noise amplification in homogeneous regions. In order to surmount this well-known problem, AHE was refined to CLAHE; described[14] and summarized.[40] Complete formulation of this approach is reviewed.[41] Due to CLAHE's well performance, it[41] seeks to efficiently implement this algorithm for the enhancement of real-time image sequences in order to reduce the processing time, although Pizer *et al*. accomplished some effort.[15] In our scheme, CLAHE transform exclusively applied to normalized approximation coefficients on the first scale of decomposition to locally enhance contrast. This process causes limitation in creation of visual artifacts, lessens being sensitive to noise and protects the important high-frequency components from undesired variation. Moreover, fixed contextual regions cannot be adapted to features of different size.

In addition, although histogram techniques are attractive due to their simplicity, effectiveness and speed, they are not perfect enhancement techniques. In an attempt to achieve excellent results, CLAHE transform was utilized in combination with WT for making chest images more visual and noise robust.

For CLAHE implementation, the normalized approximation signal of chest image is divided into regions of equal sizes (8 × 8). The clip limit was set to 0.01 as default. The histogram type is specified here to Gaussian distribution. By applying uniform distribution, the images were almost opaque and soft tissue was less visible.

Normalizing and Clipping

Since the enhanced images are reconstructed from the modified approximation and details coefficients, they are processed in 3 steps [Figure 3]. The reconstructed images are normalized to be at its best in terms of dynamic range, whereas the distribution of intensities does not change. This is done using:

$$Y_{ij} = \frac{X_{ij} - \min(X)}{\max(X) - \min(X)}. \quad (2)$$

Where X is the input gray scale image matrix, and Y is the normalized output.

The output images of this step are opaque and foggy in way that the rectangular above the chest radiographs are gray while expected to be black [Figure 4]. Looking at the histogram of images, we can figure out that almost all pixels settled in the range of 100–200 gray scales and a few pixels exist out of this range as illustrated in Figure 5a. Clipping some of the highest and lowest intensities will help to handle this problem. In this paper, 0.1% of the highest and lowest intensities were clipped. The new values of intensities are found by linear interpolation between data points. After mapping the new values [Figure 5b], the image is normalized. The chest images in this phase are shown as prefinal image [Figure 6]. Histogram of the prefinal image is plotted in Figure 5c. Finally, the image is processed by morphological filters.

Morphological Filtering

Mathematical morphology is a powerful tool for processing of geometrical structures, which operates by probing the image at each pixel with an appropriate SE. Top-Hat and its

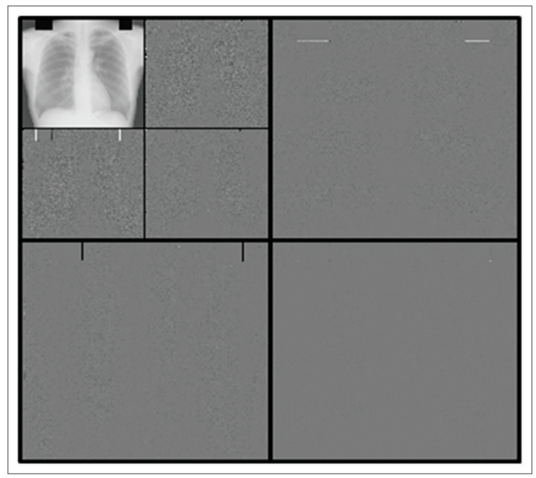

Figure 2: 2-level orthogonal wavelet decomposition of chest radiographs

Figure 3: 3 step dynamic range enhancement block diagram

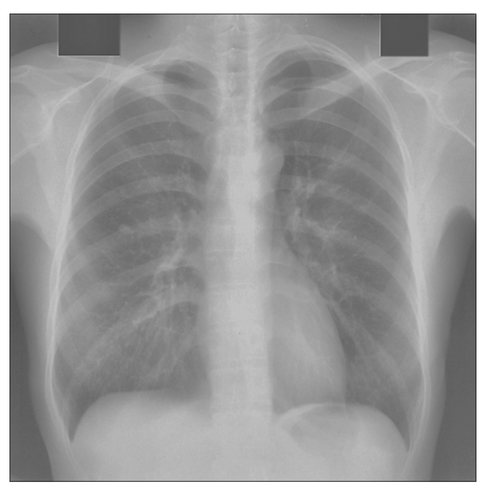

Figure 4: Normalized reconstructed image

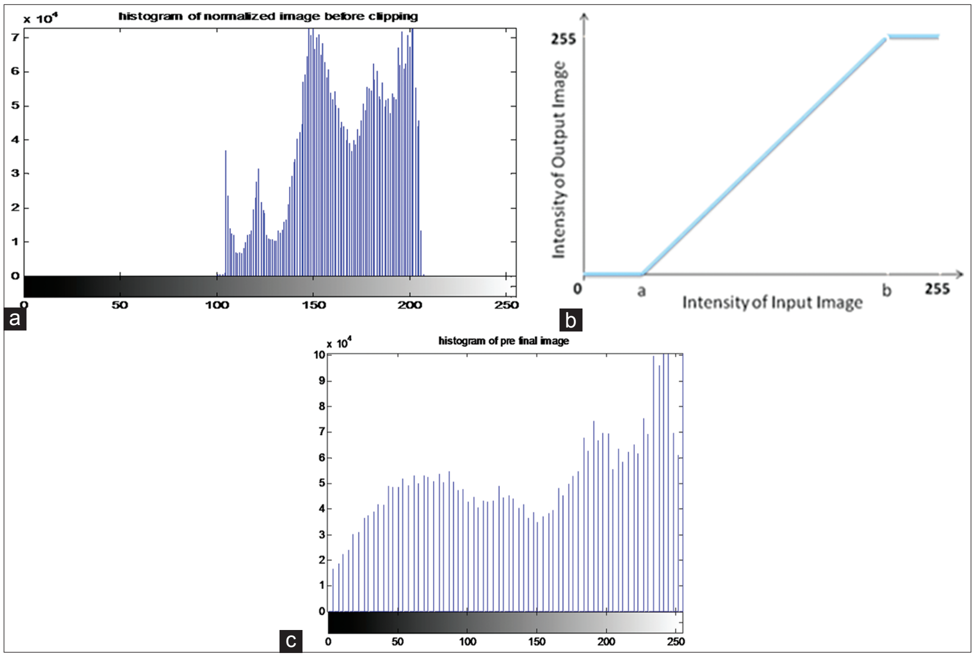

Figure 5: (a) Histogram of the normalized reconstructed image, (b) intensity remapping diagram, (c) histogram of the prefinal image

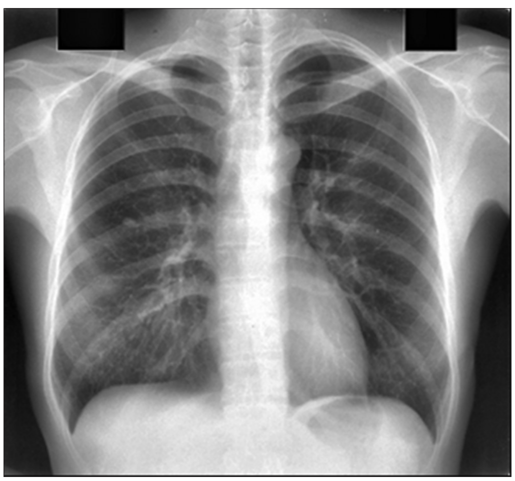

Figure 6: Prefinal image (normalized image after clipping)

dual, bottom-hat filters extract features brighter and darker than the surrounding background respectively. Indeed, a top-hat with a large isotropic SE acts as a high-pass filter.[42] It should be noted that it is done based on intensity in the spatial domain.

The procedure is adding the input chest image to the top-hat filtered image (in order to enhance bright features), then subtracting the bottom-hat filtered image (to enhance dark features) using a large disk-shaped SE. Top-Hat and bottom-hat filtering are often used together to enhance contrast using a small and equal SE. In this paper, we propose the size of SE used for bottom-hat filter to be much greater than the one used in top-hat filter. Using this method, we could adjust the image brightness and enhance the contrast notably. The SE radius is determined as 100 and 200 for top-hat and bottom-hat filter, respectively. The top-hat and bottom-hat filtered images are shown in Figure 7. Indeed, the dark features are almost strengthened twice the bright ones; considering that radiographic images are usually too bright, and lung fields are dark. At this stage, histogram of the image is almost uniform. The signal profile of the middle image line at each stage is plotted in Figure 8. The profile of the original image exhibits a gradual [Figure 8a]. The profile of the prefinal image exhibits a steep slope with a serrated edge [Figure 8b]. A serrated edge presents detail contrast which is low yet. Brighter and darker points are exhibited in the profiles of the top-hat and bottom-hat filtered images in Figure 8c and d respectively. The profile of the final enhanced image displays a steeper slope with a larger serrated edge [Figure 8e]. All the range of 0–255 gray scales are existed in this profile.

It should be cited that using large and equal SE and applying morphological filtering on the original images without the previous steps are not effective enough. Applying this step on the CLAHE transform of the original images, results in washed-out lung tissues. Using a small and equal SE (as usual) results in noisy and unsatisfactory images.

EXPERIMENTAL RESULTS AND DISCUSSION

The publicly available Japanese Society of Radiological Technology (JSRT) digital image database is used in this study. The JSRT database includes 154 conventional chest radiographs with a proven lung nodule and 93 normal cases.[43] The image size is 2048 × 2048 pixels with a spatial resolution of 0.175 mm pixel size, and 12 bits of gray scale.

In order to validate the superiority and effectiveness of the proposed method, the subjective evaluation (the visual quality of chest radiographs) were made use of as well as the objective criteria. The objective criteria include standard deviation (Std), mean, local Std, local entropy, peak signal to noise ratio (PSNR), mean square error (MSE), and contrast, derived from the gray-level co-occurrence matrix (GLCM)[44] by:

$$\text{Contrast} = \sum_{i=0}^{N-1}\sum_{j=0}^{N-1}(i-j)^2\, C(i,j)\,. \tag{3}$$

Where N is the size of the GLCM; equal to the number of gray scales. GLCMs were computed in 8 directions and up to 4 distances. Local measures were calculated according to MATLAB software (R2011a, MathWorks Inc. USA) defaults. The final values were obtained by taking the average.

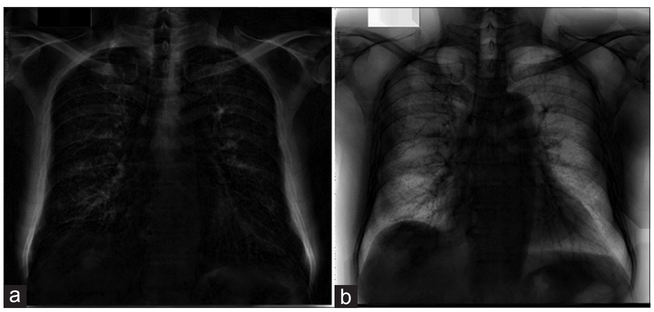

Figure 7: Top-hat and Bottom-hat filtered images: (a) top-hat filtered image, (b) bottom-hat filtered image

Standard deviation serves as a measure of image clarity and contrast. Local Std and entropy provide information about the variability of the intensity values of pixels for texture analysis. These features play a notable role in visibility of the images details. Mean represents the average brightness of images.

PSNR is defined by:

$$\text{PSNR} = 10\log_{10}\frac{255^2}{\text{MSE}}\,. \tag{4}$$

Where MSE represents the Mean Square Error between the original and the final images and is given by:

$$\text{MSE}(X_f) = \frac{1}{I\times J}\sum_{i=1}^{I}\sum_{j=1}^{J}[X_f(i,j) - X_0(i,j)]^2\,. \tag{5}$$

For an $I \times J$ image. PSNR can be viewed as a measure of quality of one of the images being compared, if the other image is considered to have perfect quality. Here, there is no image with perfect quality, so it merely indicates the degree of the similarity between original and final images.

The quantitative results for 12 typical samples of original and final chest radiographs are shown in Tables 1 and 2. Final images Std is almost twice the original one. Final images local Std is about 8 times the original one and the final images contrast is almost 7 times the original.

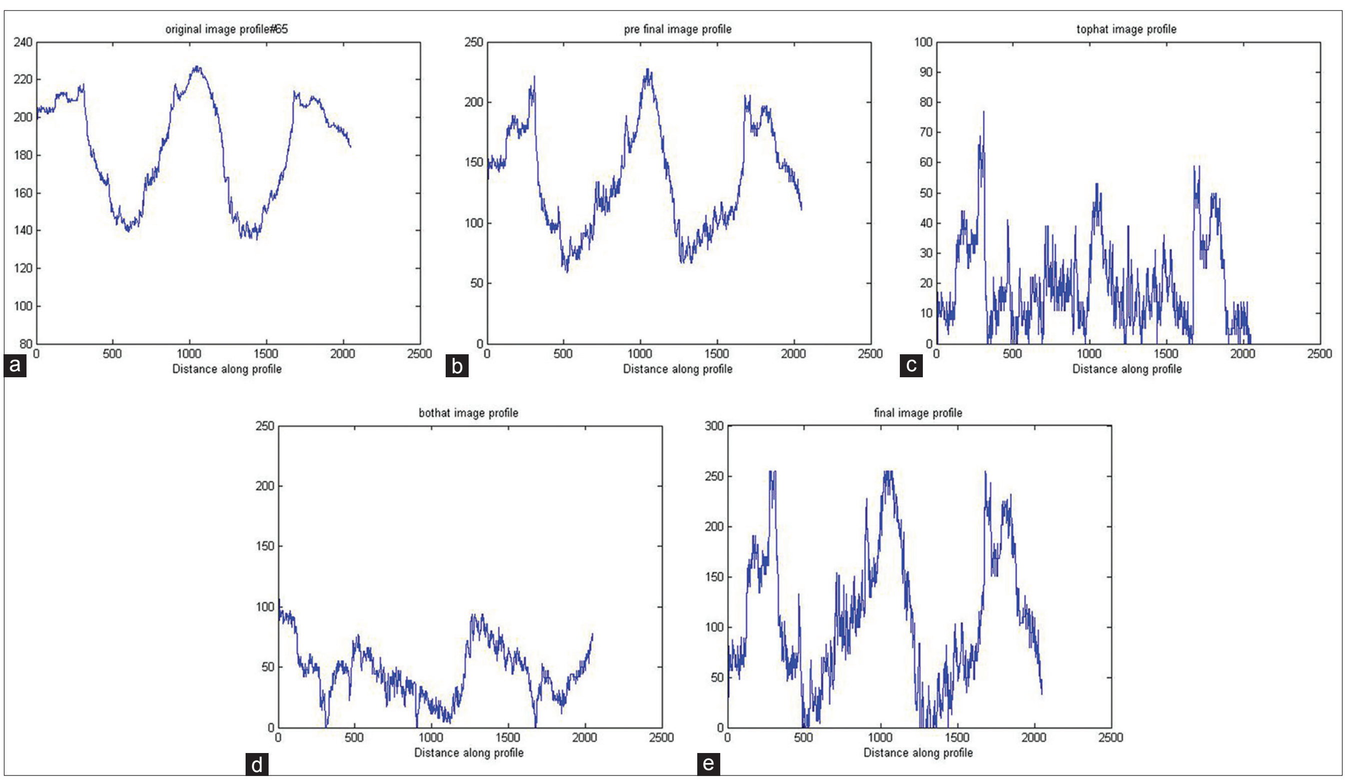

Figure 8: Signal profile of the middle image line: (a) profile of the original image. (b) Profile of the prefinal image. (c) Profiles of the top-hat filtered image. (d) Profile of the bottom-hat filtered image. (e) Profile of the final enhanced image

To demonstrate superiority of the proposed method, the performance of applying HE and CLAHE transform on the original images, our algorithm with using equal SE sizes, and the proposed methods[23,29,34] are quantified and shown in Table 3, for a typical chest radiograph of the database. The proposed method Std is the second highest value; the value for our algorithm using equal SEs being the first. The proposed method Local Std is more than 3 times the CLAHE transform one. Also, it is more than the result of our algorithm if equal SE sizes are used. The proposed method Local Entropy is also more than the algorithm using equal SEs, which may justify our choice of SEs. The proposed method contrast is also more than 3 times the CLAHE transform one.

Table 1: Quantitative results for chest radiographs images of JSRT database

Filenames	Measures					
	Std original	Std final	Mean original	Mean final	Local std original	Local std final
JPCLN001	43.9652	86.3230	197.8401	127.2516	0.7333	5.7929
JPCLN002	51.8418	86.7640	178.2612	110.7960	0.7275	5.3792
JPCLN003	41.8425	87.0031	207.6983	144.7205	0.5981	5.0051
JPCLN004	53.8779	89.2320	184.8613	136.4335	0.8200	6.2811
JPCLN005	41.5229	87.1001	211.9886	150.7277	0.5823	5.1169
JPCLN006	54.4694	86.9565	186.1226	124.8933	0.7706	5.0585
JPCLN007	44.8364	89.3721	195.3311	118.6770	0.7109	5.4464
JPCLN008	49.7670	88.2753	180.6004	124.9202	0.8272	6.3018
JPCLN009	42.7722	84.1776	206.9167	148.8956	0.6650	5.9402
JPCLN0010	47.9404	85.2392	201.0975	140.2300	0.6113	5.1852
JPCLN0011	45.2746	89.9119	177.0733	127.3190	0.7930	6.2453
JPCLN0012	33.1737	87.9812	189.4274	147.6133	0.6018	5.3406
Average	45.9403	87.3613	193.1015	133.5398	0.7034	5.5911

Std – Standard deviation; JSRT – Japanese Society of Radiological Technology

A computer with Microsoft Windows 7 × 64 (2009 edition), Intel Core i7 CPU at 2GHz, 6 GB RAM was used for the processing. The computation time of the proposed method was 14.08 s. This time is a little more than the sigmoid-transfer one and a significant amount less than the retinex one. The least amounts belong to the HE, CLAHE and the unsharp masking technique.[23] Since precision is more important than speed in this special medical application, the proposed method may outperform the compared one based on its generally better performance.

Visual evaluations were also performed by specialist radiologists in Gharazi Hospital, Isfahan, Iran. They believed that the view of the images was truly improved. It should be mentioned that among all, the soft tissue was shown specifically more distinguishable than before. Figures 9-11 illustrate three samples of original and final chest radiographs. Histogram of the images was also plotted in

Table 2: Quantitative results for chest radiographs images of JSRT database

Filenames	Measures					
	Contrast original	Contrast final	Local entropy original	Local entropy final	PSNR (db)	MSE
JPCLN001	0.0396	0.2649	1.9640	2.1499	8.7736	8.6242e+003
JPCLN002	0.0413	0.2466	2.0566	1.9683	9.3520	7.5488e+003
JPCLN003	0.0306	0.2226	1.6599	2.2299	9.5075	7.2834e+003
JPCLN004	0.0384	0.2781	2.1097	2.5811	10.6893	5.5482e+003
JPCLN005	0.0321	0.2372	1.5351	1.8614	9.5955	7.1372e+003
JPCLN006	0.0431	0.2359	1.9890	2.2246	9.9266	6.6134e+003
JPCLN007	0.0371	0.2403	1.9423	1.9329	8.3426	9.5240e+003
JPCLN008	0.0434	0.2830	2.1665	2.4409	10.0483	6.4306e+003
JPCLN009	0.0345	0.2797	1.7495	2.5136	9.9610	6.5611e+003
JPCLN0010	0.0354	0.2337	1.6865	2.6211	9.9698	6.5479e+003
JPCLN0011	0.0425	0.3009	2.1525	2.5852	10.4108	5.9157e+003
JPCLN0012	0.0343	0.2605	1.6500	2.3496	10.5279	5.7582e+003
Average	0.0377	0.2569	1.8885	2.2882	9.7587	6.9577e+003

PSNR – Peak signal to noise ratio; MSE – Mean square error; JSRT – Japanese Society of Radiological Technology

Table 3: Quantitative comparison of results

Methods	Measures						
	Std	Mean	Local std	Local entropy	Contrast	PSNR	Computation time (s)
MSR[29]	11.0976	214.4569	0.1533	0.3799	0.0052	16.3187	46.120409
Sigmoid-transfer[34]	32.4652	203.0529	0.5158	1.4935	0.0210	27.6482	10.612113
Unsharp masking[23]	56.0808	180.8753	1.8598	1.5116	0.0852	17.1405	0.978574
HE	74.7224	127.4340	1.2838	1.0154	0.0586	8.9482	0.381415
CLAHE	60.3117	184.1852	1.5122	2.0955	0.0728	17.5609	0.566596
Our algorithm with equal SE	91.3730	157.1996	4.4282	1.9090	0.2014	10.0412	17.021390
Proposed method	87.0031	144.7205	5.0051	2.2299	0.2226	9.5075	14.080369

MSR – Multi-scale retinex; CLAHE – Contrast limited adaptive histogram equalization; Std – Standard deviation; PSNR – Peak signal to noise ratio; HE – Histogram equalization; SE – Structuring element

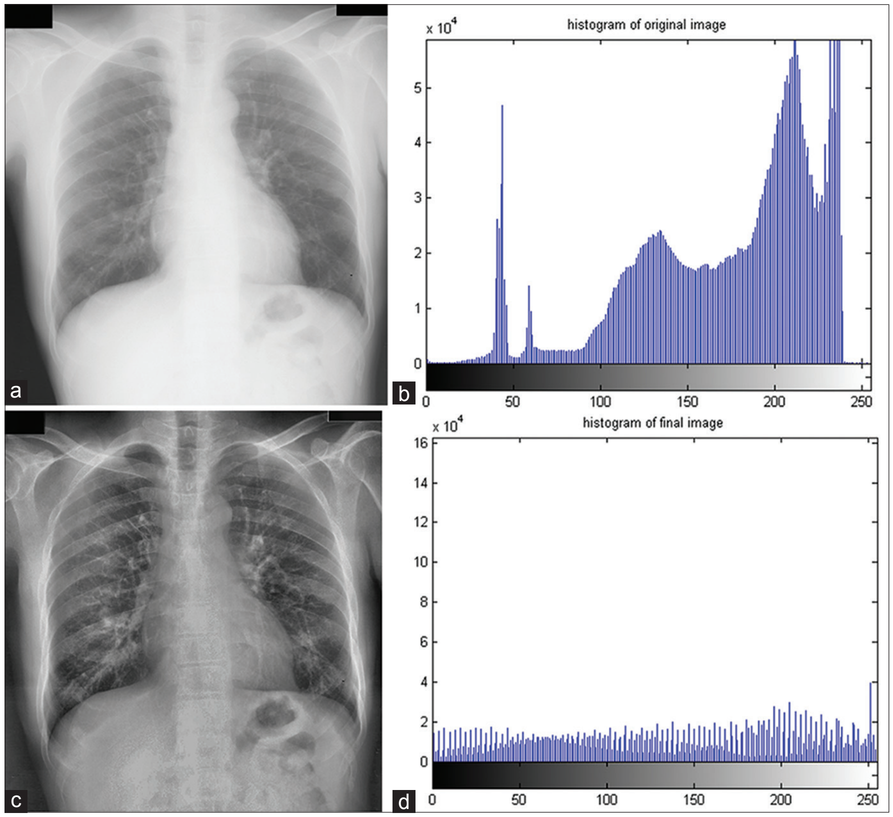

Figure 9: 67-year-old man with tuberculoma nodule: (a) Original chest radiograph image, (b) histogram of the original image, (c) the final enhanced chest radiograph image, (d) histogram of the final image

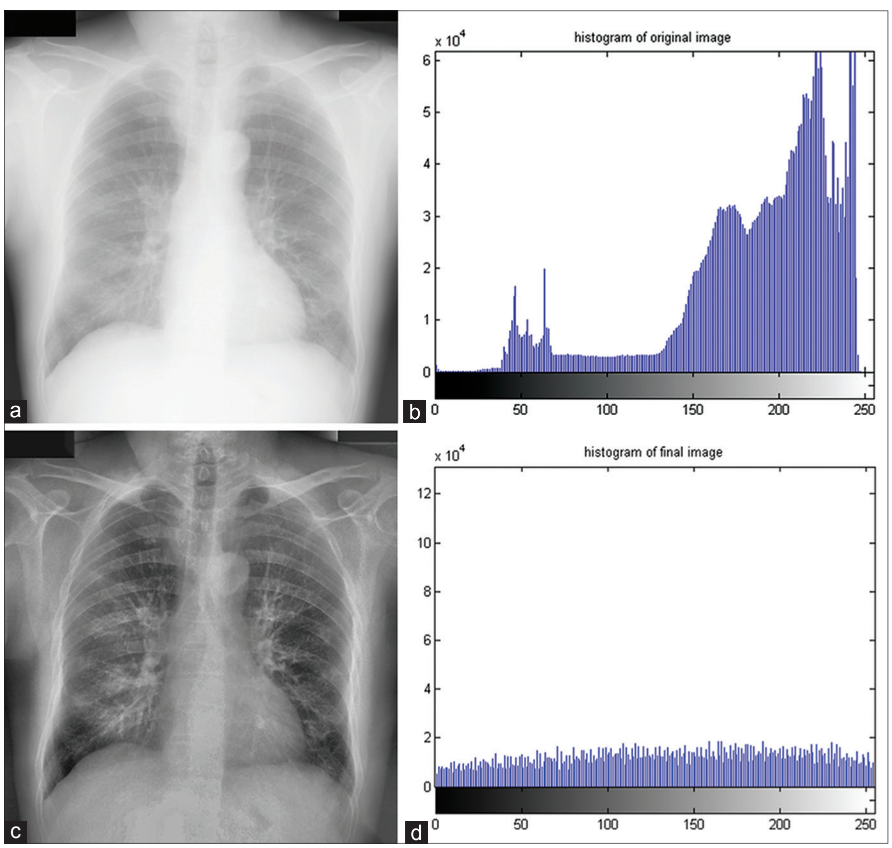

Figure 10: 56-year-old man with susp. hamartoma nodule: (a) Original chest radiograph image, (b) histogram of the original image, (c) the final enhanced chest radiograph image, (d) histogram of the final image

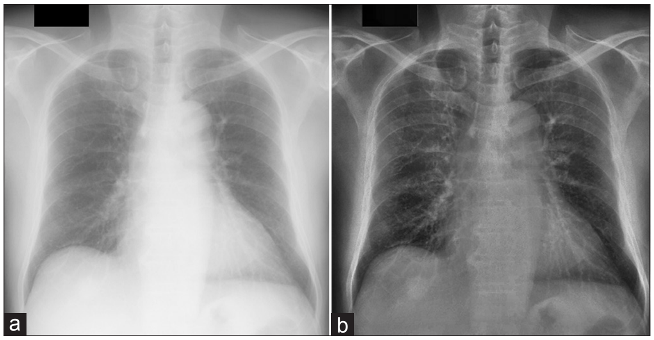

Figure 11: 64-year-old man with lung cancer: (a) Original chest radiograph image, (b) the final enhanced chest radiograph image

Figures 9 and 10. As the figures show, the overall visibility, clarity and contrast is improved remarkably and more information is available. Even the almost hidden different nodules in the original images are now extracted to an extent that is expected to help the experts in detecting them.

CONCLUSIONS

Researchers have suggested various algorithms for general and/or specific parts of chest radiographs enhancement. In order to avoid anatomical division error, in the present study, we looked for an approach which does not require any priori information, so it can be applicable to other digital radiographic images. Furthermore, the proposed method is able to appropriately enhance the entire image in a way that the initial information and natural look is preserved. We obtained satisfactory results evaluated with objective and subjective criteria. According to quantitative results, the image parameters, especially the contrast, are significantly improved. The proposed method has the capacity to be performed effectively and efficiently since the implementation of algorithm is simple and global. Although, the proposed method is not the fastest, it outperforms the compared ones, based on its better performance and relatively acceptable complexity and speed.

REFERENCES

1. van Ginneken B, ter Haar Romeny BM, Viergever MA. Computer-aided diagnosis in chest radiography: A survey. IEEE Trans Med Imaging 2001;20:1228-41.
2. McAdams HP, Samei E, Dobbins J 3rd, Tourassi GD, Ravin CE. Recent advances in chest radiography. Radiology 2006;241:663-83.
3. Sherrier RH, Chiles C, Wilkinson WE, Johnson GA, Ravin CE. Effects of image processing on nodule detection rates in digitized chest radiographs: ROC study of observer performance. Radiology 1988;166:447-50.
4. Sherrier RH, Johnson GA. Regionally adaptive histogram equalization of the chest. IEEE Trans Med Imaging 1987;6:1-7.
5. Shi Z, He L, Nakamura T, Itoh H. Enhancement of Chest Radiograph Based on Wavelet Transform. Proceeding ISNN 2009 Proceedings of the 6th International Symposium on Neural Networks: Advances in Neural Networks-Part III. 5553. 2009. p. 675-83.
6. He Q, He W, Wang K, Ma D. Effect of multiscale processing in digital chest radiography on automated detection of lung nodule with a computer assistance system. J Digit Imaging 2008;21 Suppl 1:S164-70.
7. Gonzalez RC, Woods RE. Digital Image Processing. Ch. 4. MA, Addison-Wesley Publishing Company; 1992.
8. Hummel RA. Image enhancement by histogram transformation. Comput Graphics Image Process 1977;6:18495.
9. Hall EH. Almost uniform distribution for computer image enhancement. IEEE Trans Comput 1974;23:207-8.
10. Kim YT. Contrast enhancement using brightness preserving bi-histogram equalization. IEEE Trans Consum Electron 1997; 43: 1-8.
11. Wongsritong K, Kittayaruasiriwat K, Cheevasuvit F, Dejhan K, Somboonkaew A. Contrast enhancement using multipeak histogram equalization with brightness preserving. Circuits Syst IEEE Asian Pac Conf Circuits Syst 1998;1:455-8.
12. Menotti D, Najman L, Facon J, de Araújo AA. Multi-histogram equalization methods for contrast enhancement and brightness preserving. IEEE Trans Consum Electron 2007; 53: 1186-1194.
13. Pizer SM, Zimmerman JB, Staab EV. Adaptive grey level assignment in CT scan display. J Comput Assist Tomogr 1984;8:300-5.
14. Pizer SM, Amburn EP, Austin JD, Cromartie R, Geselowitz A, Greer T, *et al*. Adaptive histogram equalization and its variations. Comput Vis Graphics Image Process 1987;39:35568.
15. Pizer SM, Johnston RE, Eriksen JP, Yankaskas BC, Muller KE. Contrast-limited adaptive histogram equalization: Speed and effectiveness. Proceedings of the 1st Conference On Visualization Biomedical Computing; 1990. p. 337-45.
16. Pisano ED, Zong S, Hemminger BM, DeLuca M, Johnston RE, Muller K, *et al.* Contrast limited adaptive histogram equalization image processing to improve the detection of simulated spiculations in dense mammograms. J Digit Imaging 1998;11:193-200.
17. Rehm K, Dallas WJ. Artifact Suppression in digital chest radiographs enhanced with adaptive histogram equalization. Proc SPIE Med Imaging 1989;III: 294-6.
18. Shuyue C, Honghua H, Yanjun Z, Xiaomin X. Study of automatic enhancement for chest radiograph. J Digit Imaging 2006;19:371-5.
19. Senthilkumar R, Senthilmurugan M. Triad histogram to enhance chest X-ray image. Int J Adv Res Comput Commun Eng 2014;3:8577-80.
20. Sezn MI, Teklap AM, Schaetzing R. Automatic anatomically selective image enhancement in digital chest radiography. IEEE Trans Med Imaging 1989;8:154-62.
21. Tahoces PG, Correa J, Souto M, Gonzalez C, Gomez L, Vidal JJ. Enhancement of chest and breast radiographs by automatic spatial filtering. IEEE Trans Med Imaging 1991;10:330-5.
22. Souto M, Correa J, Tahoces PG, Tucker D, Malagari KS, Vidal JJ, *et al.* Enhancement of chest images by automatic adaptive spatial filtering. J Digit Imaging 1992;5:223-9.
23. Saleh SH, Nordin AJ. Improving diagnostic viewing of medical images using enhancement algorithms. J Comput Sci 2011;7:1831-8.
24. Sarage GN, Jambhorkar S. Enhancement of chest X-ray images using filtering techniques. Int J Adv Res Comput Sci Softw Eng 2012;2:308-12.
25. Kwan BY, Kwan HK. Improved lung nodule visualization on chest radiographs using digital filtering and contrast enhancement. World Acad Sci Eng Technol 2011;110:590-3.
26. Tsubamoto M, Johkoh T, Kozuka T, Tomiyama N, Hamada S, Honda O, *et al.* Temporal subtraction for the detection of hazy pulmonary opacities on chest radiography. AJR Am J Roentgenol 2002;179:467-71.
27. Bao C, Sheng C. A parameterized logarithmic image processing method based on Laplacian of Gaussian filtering for lung nodules enhancement in chest radiographs. Instrumentation and Measurement, Sensor Network and Automation (IMSNA), 2013 2nd International Symposium on; 2013. p. 649-52.
28. Shi Z, Zhao M, Wang Y, He L, Suzzuki K, Jin C, *et al*. Hessian-LoG: A novel dot enhancement filter. ICIC Exp Lett 2012;6:1987-92.

29. Shuyue C, Ling Z. Chest Radiographic image enhancement based on multi-scale retinex technique. Int Conf Bioinformatics Biomed Eng 2009;1:1-3.
30. Tsai DY, Lee Y, Sekiya M, Sakaguchi S, Yamada I. A Method of Medical Image Enhancement Using Wavelet Analysis. Vol. 1. Proc. ICSP'02 Sixth International Conference on Signal Processing; 2002. p. 723-6.
31. Yan Y, Dong Z. Contrast enhancement of radiographs using shift invariant wavelet transform. Wuhan Univ J Nat Sci 2000;5:059-62.
32. Qktem H, Egiazarian K, Niittylahti J, Lemmetti J. An approach to adaptive enhancement of diagnostic X-ray images. EURASIP J Appl Signal Processing 2003;5:430-6.
33. Matozaki T, Tanishita A, Ikeguchi T. Image enhancement of chest radiography using wavelet analysis. Annu Int Conf IEEE Eng Med Biol Soc 1996;3:1109-10.
34. Lee Y, Tsai DY, Suzuki T. Contrast enhancement of medical images using sigmoid-type transfer curves for wavelet coefficient weighting adjustment. Med Image Inf Sci 2008;25:48-53.
35. Lin JS, Lo SC, Li H, Freedman MT, Mun SK. Region-based enhancement of digital chest radiographs. Proc Int Conf Acoust Speech Signal Processing 1996;7:2211-2214.
36. Vuysteke P, Schoeters E. Multiscale image contrast amplification (MUSICA). SPIE Image Processing 1994;2167:551-60.
37. Mehta IC, Khan ZJ, Khotpal RR. Analysis and review of chest radiograph enhancement techniques. Inf Technol J 2006;5:577-82.
38. Daubechies I. Ten Lectures on Wavelets. Vol. 61. Philadelphia: Proceedings CBMS-NSF Regional Conference Series in Applied Mathematics, SIAM; Society for Industrial and Applied Mathematics; 1 edition; 1992.
39. Chang SG, Yu B, Vetterli M. Adaptive wavelet thresholding for image denoising and compression. IEEE Trans Image Process 2000;9:1532-46.
40. Zuiderveld K. Contrast limited adaptive histogram equalization. In: Heckbert P, editor. Graphic Gems IV. San Diego: Academic Press Professional; 1994. p. 474-85.
41. Reza AM. Realization of the contrast limited adaptive histogram equalization (CLAHE) for real-time image enhancement. J VLSI Signal Processing 2004;38:35-44.
42. Jähne B, Haussecker H. Computer Vision and Applications: A Guide for Students and Practitioners. San Diego;Academic Press, 2000. p. 679.
43. Shiraishi J, Katsuragawa S, Ikezoe J, Matsumoto T, Kobayashi T, Komatsu K, *et al.* Development of a digital image database for chest radiographs with and without a lung nodule: Receiver operating characteristic analysis of radiologists' detection of pulmonary nodules. AJR Am J Roentgenol 2000;174:71-4.
44. Haralick RM, Shanmugan K, Dinstein I. Textural features for image classification. IEEE Trans Syst Man Cybern 1973;SMC-3:610-21.

How to cite this article: Alavijeh FS, Mahdavi-Nasab H. Multi-scale Morphological Image Enhancement of Chest Radiographs by a Hybrid Scheme. J Med Sign Sence 2015;5:59-68.

Source of Support: Nil, **Conflict of Interest:** None declared

BIOGRAPHIES

Fatemeh Shahsavari Alavijeh Received the BSc degree from Najafabad Branch, Islamic Azad university, Iran, in 2009, and the MSc degree from Azad university of Najafabad, Iran, in 2014 both in Communication Engineering. Her research interests are in image processing and computer vision systems.

E-mail: shahsavari@sel.iaun.ac.ir

Homayoun Mahdavi-Nasab Received BSc and MSc degrees from Isfahan University of Technology in Electronics and Communication Engineering in 1988 and 1993 respectively, and a PhD in Communication from Tehran, Science and Research Branch, Islamic Azad University in 2006. He is now with the Department of Electrical Engineering, Najafabad Branch of IAU as an Assistant Professor. His research interests include signal image and video processing and related soft-computing intelligent systems.

E-mail: mahdavinasab@iaun.ac.ir